
Proceedings Paper:
Reeves-McLaren, N. orcid.org/0000-0002-1061-1230, Hong, M., Alqurashi, H. et al. (4 more authors) (2018) The Spinel LiCoMnO4: 5V cathode and conversion anode. In: Energy Procedia. 3rd Annual Conference in Energy Storage and Its Applications, 11-12 Sep 2018, Sheffield, UK. Elsevier , pp. 158-162.

https://doi.org/10.1016/j.egypro.2018.09.041

Available online at www.sciencedirect.com

ScienceDirect

Energy Procedia 151 (2018) 158–162

Energy Procedia

www.elsevier.com/locate/procedia

3rd Annual Conference in Energy Storage and Its Applications, 3rd CDT-ESA-AC, 11–12 September 2018, Sheffield, UK

The Spinel $LiCoMnO_4$: 5V Cathode and Conversion Anode

Nik Reeves-McLaren[a,*], Ma Hong[a], Hazzaa Alqurashi[a], Lu Xue[a], Joanne Sharp, Anthony J. Rennie,[b] Rebecca Boston[a]

[a] *Department of Materials Science and Engineering, University of Sheffield, Sheffield, S1 3JD, UK.*
[b] *Department of Chemical and Biological Engineering, University of Sheffield, Sheffield, S1 3JD, UK*

Abstract

$LiCoMnO_4$ was made at 550 °C in 2 h using a novel biotemplating synthetic methodology. High temperature heat treatment under flowing N_2 was then used to prepare the cation-disordered rock salt, $LiCoMnO_3$. We demonstrate for the first time that both phases can operate as conversion anodes in lithium-ion batteries, operating at ~ 0.7 V with specific capacities of ~ 400 mAh g^{-1}. We also demonstrate that 1,3-propane sultone can be used as an electrolytic additive to provide a modest boost to specific capacity in cells cycled at high potentials with $LiCoMnO_4$ as the cathode.

Selection and peer-review under responsibility of the 3rd Annual Conference in Energy Storage and Its Applications, 3rd CDT-ESA-AC.

Keywords: Lithium-ion batteries; high voltage cathode; conversion anode; biotemplating.

1. Introduction

Lithium-ion batteries (LIBs) are ubiquitous in modern society, but to meet future demands higher energy density cathode and anode materials must be developed. There are exciting developments in improving specific capacities, *e.g.* accessing oxygen redox reactions,[1] but an alternative approach is increasing the cell's operational voltage. 'High voltage' materials with the spinel crystal structure reversibly (de)intercalate lithium at, or close to, 5 V *vs.* Li/Li^+, significantly higher than commercialized materials, *e.g.* $LiNi_xMn_yCo_zO_2$ ('NMC', ~ 3.7 V), or $LiFePO_4$ (3.2 V). Such spinels are often based on $LiMn_{2-x}M_xO_4$, where M can be *e.g.* Ni (4.7 V), Cr (4.8 V) or Fe (4.9 V). $LiCo_{0.5}Mn_{1.5}O_4$ was the first to breach the 5 V barrier, with deintercalation over two voltage plateaus including 40 mAh g^{-1} at ~ 5.0 V.[2]

* Corresponding author. Tel.: +44-114-222-6013. *E-mail address:* n.reeves@sheffield.ac.uk

Selection and peer-review under responsibility of the 3rd Annual Conference in Energy Storage and Its Applications, 3rd CDT-ESA-AC.
10.1016/j.egypro.2018.09.041

The first '5 V' class material was $LiCoMnO_4$, with reported discharge capacity of ~ 95 mAh g^{-1} at 5.0 V; the theoretical maximum achievable capacity for this compound is 145 mA g^{-1}.[3] It is possible to reversibly extract all Li from the crystal lattice,[4] with only ~ 0.7% change in lattice parameter.[5] This excellent dimensional stability makes $LiCoMnO_4$ a leading candidate for all-solid-state battery applications, a rapidly growing research area of substantial commercial interest. For adoption of $LiCoMnO_4$ in current cell designs, two issues must be resolved.

Firstly, synthesis of single-phase fully oxygenated $LiCoMnO_4$ is problematic, as the material loses significant amounts of oxygen on heating above 600 °C to form a cation-disordered $LiCoMnO_3$ rock salt phase at ~ 1050 °C.[6] Most synthetic approaches require calcination at ~ 800 °C, thus producing partially deoxygenated spinels that exhibit an additional lower voltage redox reaction at ~ 4 V and reduced capacity at 5 V.[7, 8] New synthetic approaches are required to maximize available specific capacity and operational voltages in fully oxygenated $LiCoMnO_4$.

Secondly, high voltage materials suffer from significant capacity fading when used with liquid electrolytes above ~ 4.7 V due to electrolytic decomposition. Some electrolytic additives have been studied, *e.g.* vinylene carbonate, 1,3-propane sultone (PS) and methylene methane disulfonate.[9-11] Additives can help prevent salt consumption, gas evolution and detrimental increases in cell impedance during cycling. Works have focused on *e.g.* extending the upper operating potential and preventing capacity fading in NMC and $Li_2NiMn_3O_8$. To our knowledge, their application has not been reported in a 5 V class material, *i.e.* $LiCoMnO_4$.

There is also a need for anode materials with increased specific capacity and lower potentials vs Li/Li^+; commercial cells currently use graphite with maximum capacities of 372 mAh g^{-1}. Attention has focused on alloying (*e.g.* Si) and intercalation (*e.g.* $Li_4Ti_5O_{12}$) anodes as potential replacements; a third option is the use of metal oxide conversion anodes.[12-14] In these, lithium insertion causes complete reduction of the metal oxide to form a mixture of metallic nanoparticles and Li_2O; the lithium can then be extracted during charge, with concomitant reoxidation of the metal. Co_3O_4 and CoO, for example, show initial capacities of ~1000 and ~ 700 mAh g^{-1} on first discharge respectively.[12] Conversion anodes typically show a large drop in capacity after first discharge but good retention thereafter.

Here, we highlight new low temperature synthetic pathways for $LiCoMnO_4$ and $LiCoMnO_3$, and report on the use of (i) PS in reducing capacity fading in $LiCoMnO_4$ as a high voltage cathode, and (ii) $LiCoMnO_4$ and $LiCoMnO_3$ as conversion anodes.

2. Experimental

$LiCoMnO_4$ was made via two different synthetic regimes, based on (i) high temperature solid state reaction ('SSR-$LiCoMnO_4$'), and (ii) a lower-temperature biotemplating ('BIO-$LiCoMnO_4$') regime, similar to that in Zilinskaite *et al.,*[15] to minimize risk of lithium and oxygen loss during reaction. Reagents were from Sigma-Aldrich, 98+% purity.

SSR-$LiCoMnO_4$ samples were made by mixing stoichiometric amounts of $Co(NO_3)_2.6H_2O$, Li_2CO_3 (dried at 180 °C) and $(CH_3CO_2)_2Mn.4H_2O$ in an agate mortar and pestle. Samples were heated in an alumina crucible to 210 °C at 0.5 °C min^{-1} to remove water and acetate/nitrates, decarbonated at 650 °C for 3 h, then reacted at 800 °C for 45 h with intermittent regrinding to complete reaction. After the final reaction, samples were annealed at 500 °C for 72 h to optimize oxygen content. For BIO-$LiCoMnO_4$ specimens, stoichiometric solutions of $CH_3COOLi.2H_2O$, $(CH_3COO)_2Mn.4H_2O$ and $(CH_3COO)_2Co.4H_2O$ in water were mixed with 10 wt% dextran. After mixing, the solutions were dried at 80 °C and heated in a muffle furnace in air at 10 °C min^{-1} to 550 °C, and calcined for 2 h.

$LiCoMnO_3$ was prepared by taking aliquots of BIO-$LiCoMnO_4$ and heating on gold foil at 950 °C for 8 h in a horizontal tube furnace under flowing N_2. Heating / cooling rates of 5 °C min^{-1} were used.

X-ray diffraction (XRD) used a Bruker D2 Phaser with Cu Kα radiation. Data analysis used the 2018 ICDD PDF-4+ database and SIeve+ software. Scanning electron microscopy (SEM) used a Phillips Inspect F on powder specimens on conductive carbon tape, coated with 15 nm thick Au. Digitized micrographs were analyzed in ImageJ.[16]

Electrodes were prepared by mixing 80 wt% active material with 10 wt% each PVdF binder and Super C45 (Imerys Graphite & Carbon) into a slurry with 1-methyl-2-pyrrolidone (anhydrous 99.5%, Sigma-Aldrich). This was cast on to carbon coated Al foil, dried, and calendared to ~ 70 μm thickness. Stainless steel (2032) coin cells were assembled under Ar in a glovebox by layering a stainless steel spacer, a prepared 12 mm electrode disc, an electrolyte-soaked glass fiber separator, and a freshly cut lithium metal disc. For cathode tests, three electrolyte solutions were tested with 1M $LiPF_6$ dissolved in (i) EC:DEC, (ii) EC:DMC, and (iii) EC:DMC with 2 wt% 1,3-propane sultone (PS, 99%, Sigma-Aldrich). Anode testing used 1 M $LiPF_6$ in EC:DMC:DEC (99%, Sigma-Aldrich) electrolyte.

Electrochemical tests were made on multiple cells for each material at 25 °C using a Maccor Series 4000 Battery Cycler; references to voltage/potential are relative to Li/Li^+. Tests studied performance of $LiCoMnO_4$ and $LiCoMnO_3$ as either cathode or conversion anode materials; comparative tests were conducted using commercial $Li_4Ti_5O_{12}$ (MTI).

3. Results and Discussion

XRD data, Fig. 1, confirm that single phase specimens of $LiCoMnO_4$ had been prepared via both solid state and biotemplated routes. In both cases, all observed Bragg peaks were indexed on the $Fd\bar{3}m$ space group. Literature reports[8] show that the lattice parameter for $LiCoMnO_{4-\delta}$ is sensitive to small changes in oxygen content, with $a \approx$ 8.05-8.06 Å for fully oxygenated specimens. Lattice parameters of 8.0587 (6) Å and 8.0691 (9) Å were refined for BIO-$LiCoMnO_4$ and SSR-$LiCoMnO_4$, respectively, suggesting the latter may be slightly oxygen deficient.

For spinels, the (220) peak is sensitive to cationic occupancy of the 8*a* tetrahedral site; effectively zero intensity is expected for a fully normal spinel with only weakly scattering Li located at this position. Our data, Fig. 1, show this to be the case for the SSR sample, but the biotemplated specimen shows a small (220) reflection at ~ 31.5 °2θ, suggesting a small amount of cation mixing is occurring, with a heavier scatterer (*i.e.* Co and/or Mn) partially swapping positions with the tetrahedral Li. The Bragg peaks are also considerably broader for the biotemplated specimen, most likely due to reduced crystallite size relative to those produced via SSR.

A sample of BIO-$LiCoMnO_4$ was extracted and heated at 950 °C under N_2. XRD data, Fig. 1, from the product were indexed on the $Fm\bar{3}m$ space group, a = 4.0260 (9) Å, consistent with previous reports on $LiCoMnO_3$.[6, 8]

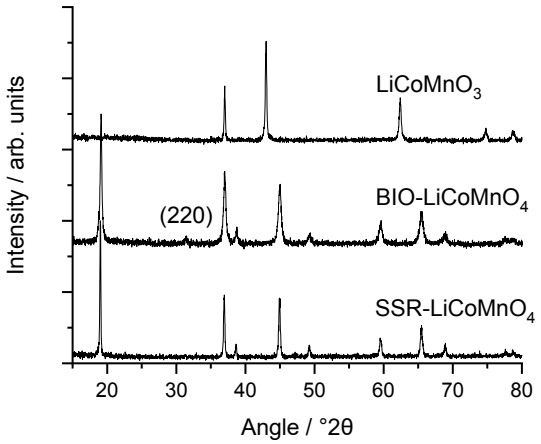

Figure 1. XRD data for SSR-$LiCoMnO_4$, BIO-$LiCoMnO_4$, and $LiCoMnO_3$. The position of the spinel (220) peak is indicated.

SEM images, Fig. 2, showed significant increases in average crystal size from ~ 0.18 (± 40) μm in the biotemplated $LiCoMnO_4$ samples growing to ~ 1.3 (± 0.5) μm in $LiCoMnO_3$ following even a short treatment at high temperatures.

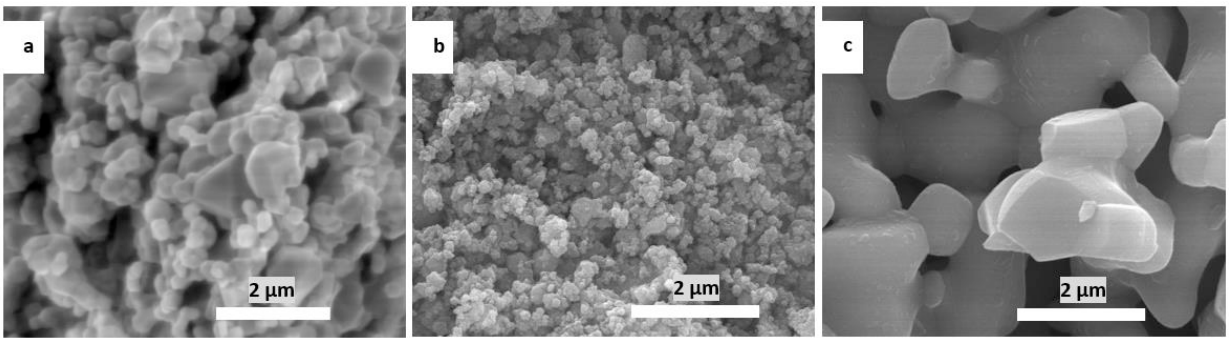

Figure 2. SEM images for (a) SSR-$LiCoMnO_4$, (b) BIO-$LiCoMnO_4$, and (c) $LiCoMnO_3$.

Charge/discharge data were collected for cells containing SSR-$LiCoMnO_4$ and three different electrolyte solutions. Cells were cycled at C/10 rate in the voltage range 3.0 to 5.3 V for 20 cycles. Example data for cells constructed using EC:DMC with 2 wt% PS electrolyte solution are shown in Fig. 3. The charge-discharge profiles can be divided into three regimes. Firstly, a small plateau of < 10 mAh g^{-1} centered at ~ 4.0 V can be attributed to a small degree of oxygen non-stoichiometry correlated with the introduction of an additional Mn^{3+} component. We then observe two plateaus centered at ~ 5.0 V, separated by a small step function likely related to some structural reorganization during lithium (de)intercalation. Specific capacities attributed to these high voltage phenomena showed small and reproducible changes depending on the electrolyte solution used: 102.5 mAh g^{-1} for cells using EC:DEC, 108 mAh g^{-1} with EC:DMC, and the highest, 110 mAh g^{-1}, for EC:DMC with 2 wt% PS. Coulombic efficiencies improved from 54 % for cells using EC:DEC to 73 % for the other electrolyte solutions; further work to improve cycling performance is ongoing, but it is apparent that careful selection of electrolyte components is crucial in the development of cells employing high voltage cathode materials.

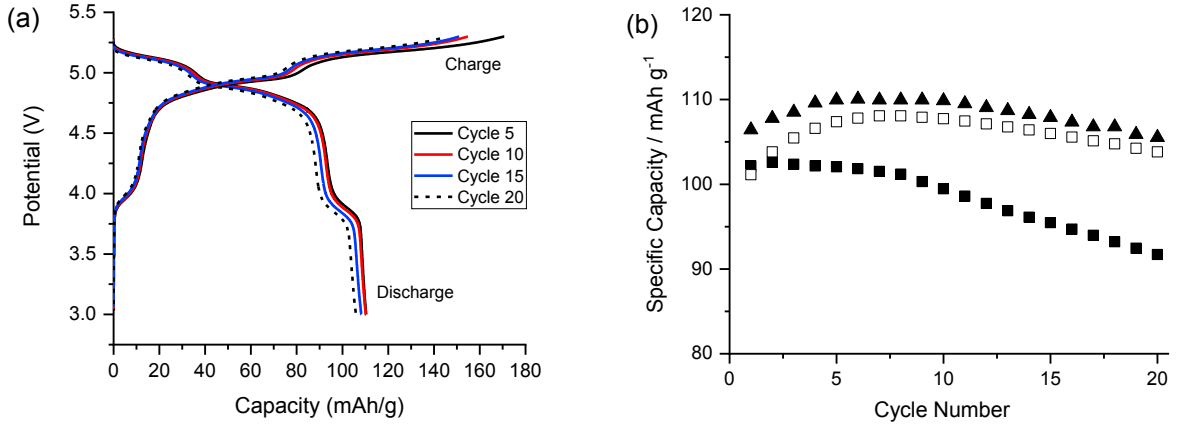

Figure 3. (a) Charge-discharge profile for $LiCoMnO_4$ with 1:1 EC:DMC with 2 wt% PS electrolyte, and (b) discharge capacities for SSR-$LiCoMnO_4$ with 1:1 EC:DEC (■), 1:1 EC:DMC (□), and 1:1 EC:DMC with 2 wt% PS (▲) cycled in the range 3.0 – 5.3 V at C/10

Negative electrodes were prepared for electrochemical testing using either $LiCoMnO_4$ or $LiCoMnO_3$ as the active material and coin cells cycled at C/5 rate in the potential range 0.25 – 2.5 V. Experimental charge/discharge data for the first two cycles are shown in Fig. 4. During the initial lithiation step, plateaus at ~ 0.7 – 0.8 V were observed with associated capacities of 1154 and 815 mAh g^{-1} for $LiCoMnO_4$ and $LiCoMnO_3$ respectively. Based on previous studies of cobalt manganate conversion anodes, the reactions occurring at this stage will involve full reduction of the metal species, likely following the reaction $LiCoMnOx + (2x–1)Li \rightarrow x\ Li_2O + Co + Mn$. Theoretical capacities, assuming

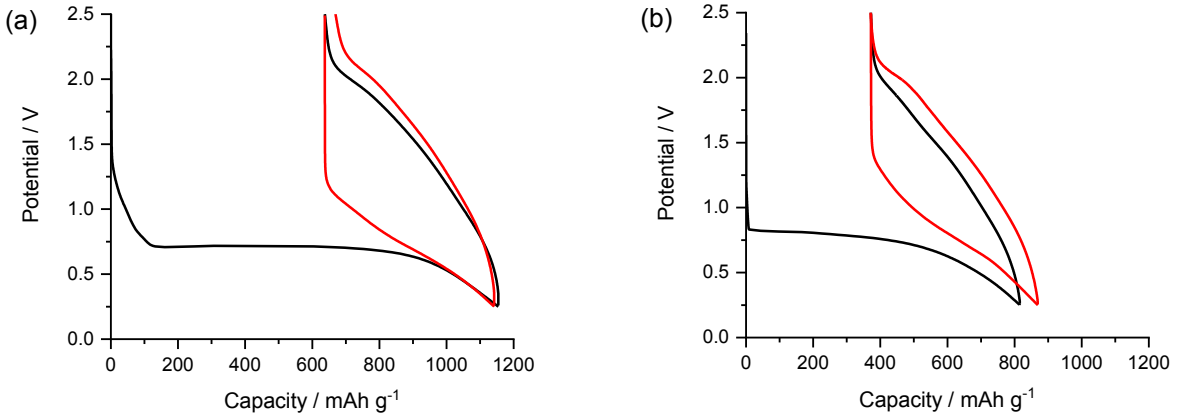

Figure 4. Charge-discharge profiles for (a) $LiCoMnO_4$ and (b) $LiCoMnO_3$ over first (black) and second (red) cycles in the range 0.25 – 2.5 V.

complete reduction can be achieved, would be 1015 mAh g^{-1} for $LiCoMnO_4$, and 790 mAh g^{-1} for $LiCoMnO_3$; excess Li is taken up during first discharge due to SEI formation. A large portion of this initial capacity is irreversible, but on further charge-discharge cycles *ca.* 400 mAh g^{-1} is reversibly cycled with reasonable retention on a more inclined potential plateau centered at ~ 0.7 V. Capacities over 10 cycles are well in excess of those observed for $Li_4Ti_5O_{12}$, Fig. 5, though further work is planned to optimize performance and improve capacity retention on cycling.

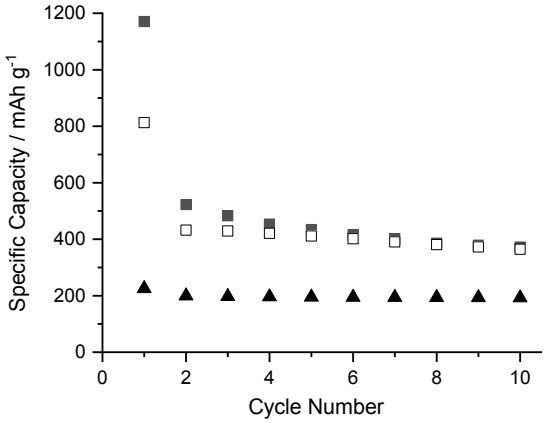

Figure 5. Discharge capacity retention for compositions BIO-$LiCoMnO_4$ (■), $LiCoMnO_3$ (□), and commercial $Li_4Ti_5O_{12}$ (MTI, ▲).

Acknowledgements

RB acknowledges that this project was supported by the Lloyd's Register Foundation and Royal Academy of Engineering under the Research Fellowships scheme.

References

[1] Luo, K., M.R. Roberts, R. Hao, N. Guerrini, D.M. Pickup, Y.-S. Liu, *et al.* Nature Chemistry. 2016;8:684.

[2] Kawai, H., M. Nagata, H. Kageyama, H. Tukamoto, A.R. West. Electrochimica Acta. 1999;45(1):315-27.

[3] Kawai, H., M. Nagata, H. Tukamoto, A.R. West. Electrochemical and Solid-State Letters. 1998;1(5):212-4.

[4] Dräger, C., F. Sigel, S. Indris, D. Mikhailova, L. Pfaffmann, M. Knapp, *et al.* Journal of Power Sources. 2017;371:55-64.

[5] Ariyoshi, K., H. Yamamoto, Y. Yamada. Electrochimica Acta. 2018;260:498-503.

[6] Reeves, N., C.A. Kirk, A.R. West. Journal of Materials Chemistry. 2001;11(2):249-50.

[7] Pasero, D., S. De Souza, N. Reeves, A.R. West. Journal of Materials Chemistry. 2005;15(41):4435-40.

[8] Reeves-McLaren, N., J. Sharp, H. Beltrán-Mir, W.M. Rainforth, A.R. West. Proceedings of the Royal Society A: Mathematical, Physical and Engineering Sciences. 2016;472(2185).

[9] Xia, J., N. Sinha, L. P. Chen, G.Y. Kim, D. Xiong, J. R. Dahn. Journal of the Electrochemical Society. 2014;161:A84-A8.

[10] Li, B., M. Xu, T. Li, W. Li, S. Hu. Electrochemistry Communications. 2012;17:92-5.

[11] Pires, J., L. Timperman, A. Castets, J.S. Pena, E. Dumont, S. Levasseur, *et al.* RSC Advances. 2015;5(52):42088-94.

[12] Poizot, P., S. Laruelle, S. Grugeon, L. Dupont, J.M. Tarascon. Nature. 2000;407:496.

[13] Badway, F., I. Plitz, S. Grugeon, S. Laruelle, M. Dollé, A.S. Gozdz, *et al.* Electrochemical and Solid-State Letters. 2002;5(6):A115-A8.

[14] Pasero, D., N. Reeves, A.R. West. Journal of Power Sources. 2005;141(1):156-8.

[15] Zilinskaite, S., A.J.R. Rennie, R. Boston, N. Reeves-Mclaren. Journal of Materials Chemistry A. 2018;6(13):5346-55.

[16] Schindelin, J., T. Rueden Curtis, C. Hiner Mark, W. Eliceiri Kevin. Molecular Reproduction and Development. 2015;82(7-8):518-29.